ORGANOMETALLICS

Article

pubs.acs.org/Organometallics

Ytterbium(III) Complexes Coordinated by Dianionic 1,4-Diazabutadiene Ligands

Boris G. Shestakov,[†] Tatyana V. Mahrova,[†] Joulia Larionova,[‡] Jêrome Long,[‡] Anton V. Cherkasov,[†] Georgy K. Fukin,[†,#] Konstantin A. Lyssenko,[§] Wolfgang Scherer,[∥] Christoph Hauf,[∥] Tatiana V. Magdesieva,[⊥] Oleg A. Levitskiy,[⊥] and Alexander A. Trifonov*[,†,§,#]

[†]G. A. Razuvaev Institute of Organometallic Chemistry of Russian Academy of Sciences, 49 Tropinina str., 603950, Nizhny Novgorod, GSP-445, Russia

[‡]Institut Charles Gerhardt Montpellier, UMR 5253 CNRS-UM2-ENSCM-UM1, Chimie Moléculaire et Organisation du Solide, Université Montpellier II, Place E. Bataillon, 34095 Montpellier cedex 5, France

[§]A. N. Nesmeyanov Institute of Organoelement Compounds of Russian Academy of Sciences, 28 Vavilova str., 119991, Moscow,GSP-1, Russia

[∥]Institute of Physics, University of Augsburg, 86135 Augsburg, Germany

[⊥]Moscow State University, GSP-1, Leninskie Gory, Moscow, 119991, Russia

[#]Nizhny Novgorod State University, 23 Gagarin av., 603950, Nizhny Novgorod, Russia

Supporting Information

ABSTRACT: A series of new Yb(III) complexes $XYb(DAD)^{2-}(L)$ (X = C_5Me_5, C_5Me_4H, $N(SiMe_3)_2$, ^tBuO; DAD = 2,6-R″$_2C_6H_3N$═C(R′)-C(R′)═NC_6H_3R″$_2$-2,6, R′ = H, Me, R″ = Me, ^{i}Pr; L = thf, dme) coordinated by redox-active diazabutadiene ligands in dianionic form were synthesized and characterized. The half-sandwich complexes $Cp^{\#}Yb(DAD)^{2-}(THF)$ ($Cp^{\#}$ = C_5Me_5, C_5Me_4H) were synthesized by the reactions of the ytterbocenes $Cp^{\#}_2Yb(THF)_2$ with the corresponding DADs in a 1:1 molar ratio. These reactions are accompanied by oxidation of the Yb(II) to Yb(III), cleavage of one $Cp^{\#}$–Yb bond, oxidation of cyclopentadienyl anion, and reduction of the diazabutadiene to dianionic form. It was found that the substituents by the DAD nitrogens (2,6-^{i}Pr$_2C_6H_3$ vs 2,6-$Me_2C_6H_3$) and imino carbons (H vs Me) do not affect the reaction outcome and afford $Cp^{\#}Yb(DAD)^{2-}$(thf). The amido and alkoxo derivatives $XYb(DAD)^{2-}$(dme) (X = $N(SiMe_3)_2$, ^tBuO) were obtained by the salt metathesis reactions of the in situ generated species $[XYbCl_2(thf)_n]$ and $Na_2(thf)_n$[2,6-^{i}Pr$_2C_6H_3$NC(Me)C(Me)-$NC_6H_3{}^iPr_2$-2,6]. If the reaction was carried out in the presence of Li ions, it afforded an ate-complex {$Li(thf)_3$}{Yb-[2,6-^{i}Pr$_2C_6H_3$NC(Me)C(Me)$NC_6H_3{}^iPr_2$-2,6]$^{2-}$[$N(SiMe_3)_2$](μ-Cl)}. The X-ray studies of complexes $XYb^{III}(DAD)^{2-}(L)$ revealed that they feature the 2σ:η^2-type of coordination of dianionic DAD ligands. Introduction of Me-substituents by the imino carbons of DADs leads to some elongation of Yb–$Cp^{\#}$ bonds compared to the NCHCHN-analogues. The Yb–C_{NCCN} bonds and the dihedral YbNN–NCCN angles were found to be the most sensitive to replacing H by Me. Unlike the formerly reported complex Cp*Yb[2,6-^{i}Pr$_2C_6H_3$NCHCHN$C_6H_3{}^iPr_2$-2,6]$^{2-}$(thf), the variable-temperature magnetic measurements (1.8–300 K) of complexes **3**–**5** and **7**–**9** did not reveal thermally induced redox isomeric transformations for these compounds. However, for complex (C_5Me_4H)Yb[2,6-^{i}Pr$_2C_6H_3$NC(Me)C(Me)$NC_6H_3{}^iPr_2$-2,6](thf) at 9 K, the structural phase transition accompanied by changes of the coordination behavior of the DAD ligand was detected, which might hint for an onset of a temperature-induced redox isomerism. These results clearly indicate high sensitivity of redox isomeric transformations of $XYb^{III}(DAD)^{2-}L$ to the smallest changes of the structural and electronic properties of the DAD ligands.

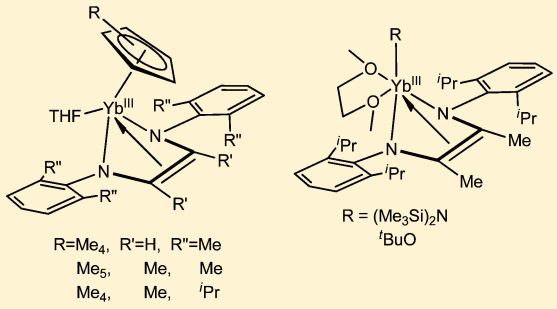

INTRODUCTION

The application of redox-active 1,4-diaza-1,3-butadiene (DAD)[1] ligands has led to the development of rich coordination and redox organolanthanide chemistry.[2] The lone electron pairs at nitrogen atoms and the π-electrons of the C═N bonds allow DAD molecules to act both as n- and π-electron donors, thus providing a variety of coordination modes. DADs can coordinate lanthanide atoms as neutral ligands[3] withal; due to their electron affinity,[4] they can oxidize electropositive Ln(II) species,[5] transforming into radical anions[3,6] or dianions[7] by accepting one or two electrons, respectively. An expansion of lanthanide

Received: November 6, 2014
Published: April 1, 2015

DOI: 10.1021/om501121s
Organometallics 2015, 34, 1177–1185

chemistry due to DAD ligands allowed for finding new phenomena in this field such as solvent-mediated redox tranformations[6c,e,f] and temperature-induced redox isomerism.[7,8] In our previous works, it was demonstrated that the redox reactions of ytterbocenes with DADs are sterically and electronically tunable. Depending on the extent of steric crowding of the coordination sphere of metal atoms and the nature of metal−ligand bonding, these reactions can occur with metal atom oxidation,[6] C−C bond formation,[9] and C−H bond activation.[9] Moreover, variation of steric saturation of the ytterbium coordination sphere allows for switching the reductive capacity of ytterbocenes in their reactions with DADs from one- to two-electron reduction.[7] The role of the steric demand of the cyclopentadienyl ligands coordinated to Yb(II) in directing redox reactions with DADs was elucidated to some extent,[7,10] while the influence of steric and electronic properties of DAD ligands still remains unclear. Hereafter, we report on the reactions of ytterbocenes $Cp^{\#}_2Yb(THF)_2$ ($Cp^{\#} = C_5Me_5$, C_5Me_4H) with the DADs having different steric and electronic properties, 2,6-$R''_2C_6H_3N{=}C(R')$-$C(R'){=}NC_6H_3R''_2$-2,6 (R′ = H, Me; R″ = Me, ^{i}Pr). Furthermore, in order to expand the series of the Yb(III) complexes coordinated by dianionic DAD ligands featuring temperature-induced redox isomeric transformations $[CpYb^{III}(DAD)^{2-}(L)] \rightleftarrows [CpYb^{II}(DAD)^{-}(L)]$[7] (L = neutral, redox innocent ligand), we synthesized a series of new compounds containing along with DAD^{2-} electron-withdrawing (compared to the electron-donating C_5Me_5[7]) amido and alkoxy groups. The structures and magnetic behavior in a wide temperature range of complexes $Cp^*Yb^{III}[R''_2C_6H_3NC(R')C(R')NC_6H_3R''_2](thf)$ (R′ = H, Me; R″ = Me, ^{i}Pr) and $RYb^{III}[2,6\text{-}^iPr_2C_6H_3NC(Me)C(Me)\text{-}NC_6H_3{}^iPr_2\text{-}2,6](dme)$ (R = $N(SiMe_3)_2$, O^{t}Bu) will be discussed also.

RESULTS AND DISCUSSION

In our previous research, it was demonstrated that the outcome of redox reactions of ytterbocenes with DADs is dependent on the steric demand of cyclopentadienyl ligands coordinated to Yb(II).[7] Thus, ytterbocene $(C_5MeH_4)_2Yb(thf)_2$ reacts with diazabutadiene 2,6-$^iPr_2C_6H_3N{=}CH\text{-}CH{=}NC_6H_3{}^iPr_2$-2,6 ($DAD^{4iPr2H}$) as a one-electron reductant to afford a bis(cyclopentadienyl) Yb(III) derivative containing a DAD radical anion $(C_5MeH_4)_2Yb^{III}(DAD^{-\cdot})$. However, ytterbocenes $Cp^{\#}_2Yb(thf)_2$ coordinated by sterically demanding cyclopentadienyl ligands act as two-electron reductants in their reactions with DAD^{4iPr2H}. These reactions occur by the abstraction and oxidation of one $Cp^{\#}$-anion, and oxidation of Yb(II) to Yb(III), and result in the formation of half-sandwich complexes $Cp^{\#}Yb^{III}(DAD^{4iPr2H})^{2-}(thf)$ ($Cp^{\#} = C_5Me_5$ (**1**), C_5Me_4H (**2**))[7] coordinated by enediamido ligands. In order to evaluate the limits of the above-mentioned synthetic approach and to elucidate the effect of steric demand of the DAD ligand, the reactions of ytterbocenes $Cp^{\#}_2Yb(thf)_2$ ($Cp = C_5Me_5$, C_5Me_4H) with less bulky 1,4-diaza-1,3-butadiene 2,6-$Me_2C_6H_3N{=}CH\text{-}CH{=}NC_6H_3Me_2$-2,6 ($DAD^{4Me2H}$) were studied (Scheme 1). The magnetic measurements for complex **1**[7] in the wide range of temperatures (2−300 K) were indicative of the existence of thermally induced redox isomerism $[CpYb^{III}(DAD)^{2-}(L)] \rightleftarrows [CpYb^{II}(DAD)^{-\cdot}(L)]$ for this compound. To elucidate the impact of the redox properties of DAD ligands on the feasibility of redox isomeric transformation, less electron-withdrawing diazabutadienes bearing by the imino carbons electron-donating Me groups 2,6-$R_2C_6H_3N{=}C(Me)\text{-}C(Me){=}NC_6H_3R_2$-2,6 (R = Me ($DAD^{4Me2Me}$), ^{i}Pr ($DAD^{4iPr2Me}$)) were tested.

Scheme 1

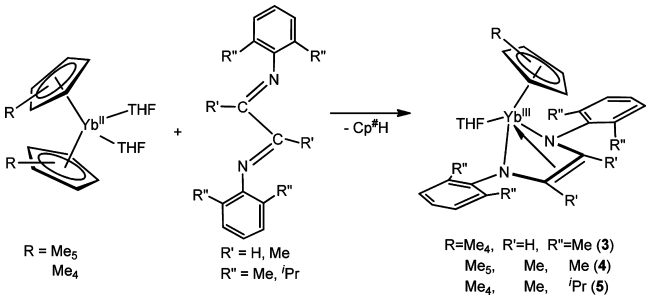

Moreover, an ascertainment of possible interconnection of the structural properties and redox behavior of complexes $Cp^{\#}Yb^{III}(DAD^{2-})(thf)$ represents a special interest.

For quantitative estimation of redox ability of the DAD ligands, as well as its dependence on the substituents at C and N atoms, voltammetric investigation of four different diazabutadienes was performed in DMF using a Pt disk electrode. Since the reduction of DAD occurs within the N=C-C=N fragment, the redox properties can be modulated by insertion of appropriate substituents. For all ligands, one-electron reduction peaks were detected (see the Supporting Information, Figure S1). The peak potential values are given in Table 1. Electron affinities within the pairs DAD^{4Me2H}, DAD^{4iPr2H} and DAD^{4Me2Me}, $DAD^{4iPr2Me}$ are similar: the difference in the reduction potential values does not exceed 30 mV. This means that redox properties of the ligand are not sensitive to the type of alkyl substituent in the phenyl ring. Unlike the small influence of the alkyl groups in the aromatic moieties, the introduction of methyl groups at the imine carbon atoms substantially influences the reduction potential values of both DAD^{4Me} and DAD^{4iPr}. Thus, DAD^{4Me2H} and DAD^{4iPr2H} are more readily reduced than their Me-substituted counterparts for approximately 400 mV. This estimation is in agreement with the literature data obtained for dimesityl substituted diazabutadienes (DAD^{MesH} and DAD^{MesMe}).[11] Electrochemical behavior of DADs was investigated[11] in acetonitrile and showed in all cases completely irreversible peaks, indicating that electron transfer is followed by a chemical follow-up step. Our results obtained in DMF showed that this solvent sufficiently increases the stability of the reduced monoanionic form of DAD, at least at the CV time scale.

Table 1. Direct (E_p^c) and Reverse (E_p^a) Peak Potential Values Observed in the Reduction of DADs (DMF, Pt, 200 mV/s, 0.05 M Bu_4NBF_4, vs Ag/AgCl/KCl)

DAD	DAD^{4Me2H}	DAD^{4iPr2H}	DAD^{4Me2Me}	$DAD^{4iPr2Me}$
$-E_p^c/E_p^a$, V	1.59	1.62/1.54	1.98	2.02/1.90

Thus, for DAD^{4iPr2H}, the reduction is quasi-reversible (the current ratio $I_c/I_a = 1$ at scan rates in the range of 50−500 mV/s; the peak separation ΔE_p is equal to 80 mV at a scan rate of 200 mV/s) and diffusionally controlled (as follows from the linear $I_p - \nu^{1/2}$ relationship, where ν is a scan rate). An insertion of methyl groups at imine carbons decreases the stability of the reduced form of $DAD^{4iPr2Me}$ even in DMF; the reverse-to-direct peak current ratio decreases to 0.4 at a scan rate of 200 mV/s. The reduction of DAD^{4Me} is irreversible, despite the nature of the substituent at the imine carbon (H or Me). Since the reduction potential values for DAD^{4Me} and DAD^{4iPr} are similar, the relative stability of the radical-anion in the latter case should be more likely attributed to steric reasons.

DOI: 10.1021/om501121s
Organometallics 2015, 34, 1177−1185

Scheme 2

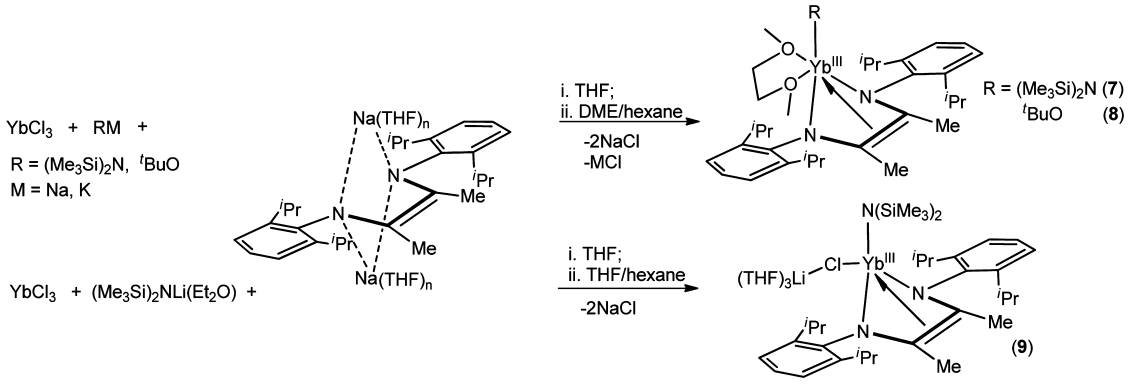

The reactions of $Cp^{\#}_2Yb(thf)_2$ with equimolar amounts of DADs (DAD^{4Me2H}, DAD^{4Me2Me}, $DAD^{4iPr2Me}$) were carried out in toluene at 50 °C (Scheme 1).

It was found that, for all tested 1,4-diaza-1,3-butadienes DAD^{4Me2H}, DAD^{4Me2Me}, and $DAD^{4iPr2Me}$, the reactions occur similarly and afford mixed-ligand Yb(III) complexes ($Cp^{\#}Yb^{III}(DAD^{2-})(thf)$ **3**–**5** (Scheme 1)) in moderate yields (49, 57, and 35%, respectively). In the case of the reaction of $(C_5Me_4H)_2Yb(thf)_2$ with $DAD^{4iPr2Me}$, the second ytterbium containing product $(C_5Me_4H)_3Yb$ (**6**) was isolated from the reaction mixture in 10% yield (for the structure of $(C_5Me_4H)_3Yb$, see Figure S2 and Table S1, Supporting Information). The formation of complex **6** apparently results from the oxidation of $(C_5Me_4H)_2Yb(thf)_2$ by a $C_5Me_4H\cdot$ radical, which appears in the reaction mixture due to oxidation of the $C_5Me_4H^-$ anion by $DAD^{4iPr2Me}$. Tedious separation of complexes **5** and **6** by fractional crystallization results in decrease of their yields. In all the attempts to detect in the reaction mixtures the $[Cp^{\#}]_2$ dimers, the expected products of transformation of the related radicals, failed. However, the GC and GC-MS methods give evidence for the presence of $Cp^{\#}H$. The formation of $Cp^{\#}H$ obviously results from the hydrogen abstraction by cyclopentadienyl radicals. The reaction solvent seems to be the most plausible source of hydrogen.

Yellowish green complexes **3**, **4**, and **5** are highly air- and moisture-sensitive, soluble in toluene, and less soluble in hexane.

Another goal of the present work was to expand the family of Yb(III) complexes coordinated by dianionic DAD ligands—prospective objects for investigation of thermally induced redox isomerism. The idea was to combine in the Yb(III) coordination sphere DAD^{2-} ligands with electron-withdrawing (compared to electron-donating $Cp^{\#}$) groups ($N(SiMe_3)_2$ and O^tBu). Although this task turned out rather difficult to realize, we succeeded to develop a synthetic approach which allowed for the synthesis of complexes $RYb^{III}(DAD^{4iPr2Me})(dme)$ (R = $N(SiMe_3)_2$ (**7**), O^tBu (**8**)) (Scheme 2). The treatment of $YbCl_3$ with equimolar amounts of $(Me_3Si)_2NNa$ or ^tBuOK in THF (60 °C, 72 h) and subsequent addition of the solution of $Na_2(THF)_x(DAD^{4iPr2Me})$ in THF (1:1 molar ratio) afforded complexes **7** and **8** after extraction of the reaction products with toluene and recrystallization from DME/hexane mixtures in 44 and 58% yields, respectively. When $(Me_3Si)_2NLi(Et_2O)$ was used instead of $(Me_3Si)_2NNa$, the reaction afforded the ate-complex $\{Li(thf)_3\}\{Yb[2,6\text{-}^iPr_2C_6H_3NC(Me)C(Me)NC_6H_3{}^iPr_2\text{-}2,6]^{2-}[N(SiMe_3)_2](\mu\text{-}Cl)\}$ (**9**) (42%) (Scheme 2). Complexes **7** (blue green), **8** (blue green), and **9** (blue green) are highly air- and moisture-sensitive, soluble in toluene, and less soluble in hexane.

X-ray Crystal Structures. Crystals of **3**–**5** suitable for single-crystal X-ray diffraction studies were obtained by continuous cooling their hexane solutions at −5 °C. The crystal structures of complexes **3**, **4**, and **7** were determined at 100(2) K and of **8**, **9** at 150(2) K. Moreover, the crystal structure of complex **5** was determined at 100(2) K and at 9(2) K; they are denoted as **5HT** and **5LT**, respectively. The molecular structures of **3**–**5** and **7**–**9** determined at 100(2) K are depicted in Figures 1–6,

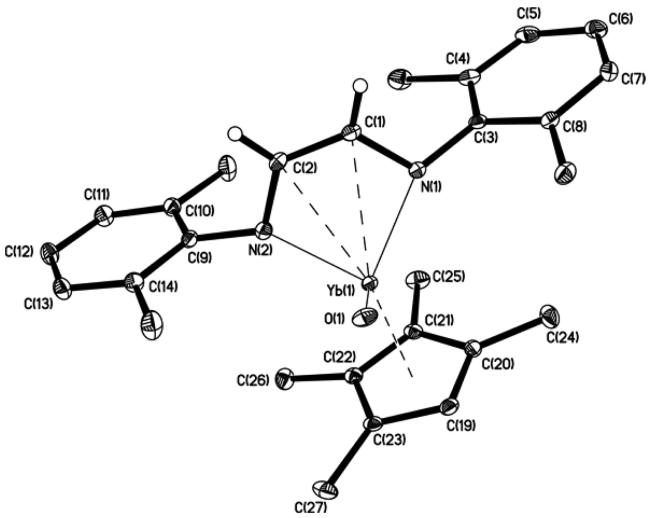

Figure 1. Molecular structure of complex **3**. Thermal ellipsoids drawn at the 30% probability level. Carbon atoms of THF molecule and hydrogen atoms are omitted for clarity.

respectively, the selected bond lengths and angles are compiled in Table 2, and crystal and structural refinement data are listed in Table S1 (see the Supporting Information).

The X-ray crystal structure determinations of **3**–**5** revealed that these complexes have structures similar to those of previously published for **1** and **2**. The coordination environment of the Yb(III) ion in complexes **3**–**5** is set up by an η^5-coordinated $Cp^{\#}$ ligand, $2\sigma{:}\eta^2$-coordinated dianion of diazabutadiene, and one THF molecule (Figures1–3).

The Yb–C($Cp^{\#}$) distances in **3**-**5HT** vary in the range of 2.586(2)–2.623(2) (**3**), 2.585(2)–2.637(2) (**4**), and 2.551(3)–2.679(3) Å (**5HT**). The average Yb–C($Cp^{\#}$) bond lengths in complex **3**-**5HT** (2.60, 2.61, and 2.62 Å, respectively) are much shorter than the corresponding values in the parent Yb(II) complexes (for comparison, see: $Cp^*_2Yb(py)_2$, 2.74 Å)[12] and clearly indicate oxidation of ytterbium during the reactions.

DOI: 10.1021/om501121s
Organometallics 2015, 34, 1177–1185

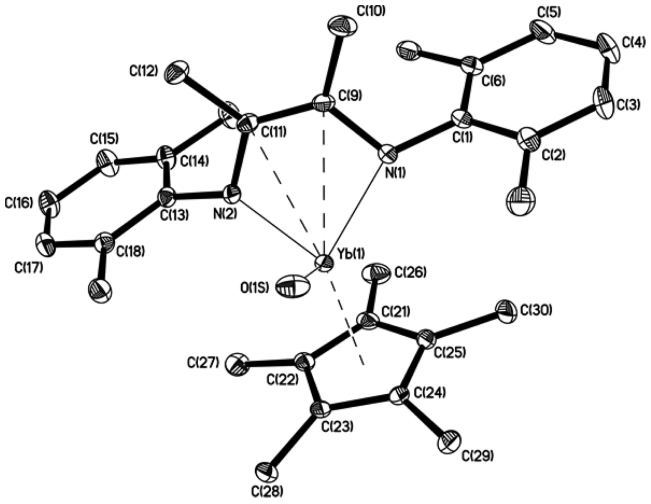

Figure 2. Molecular structure of complex **4**. Thermal ellipsoids drawn at the 30% probability level. Carbon atoms of THF molecule and hydrogen atoms are omitted for clarity.

These distances are somewhat longer compared to those in **1** and **2** (2.59 Å).[7] The Yb−N distances in **3**-**5HT** (2.151(2), 2.151(2) Å in **3**; 2.132(1), 2.152(1) Å in **4**; 2.139(2), 2.151(2) Å in **5HT**) are similar to those measured for **1** and **2** and are noticeably shorter compared to the coordination bonds in the related eight-coordinate Yb(III) complexes (2.193(1)−2.286(7) Å).[13] The lengths of N−C (1.418(3), 1.408(3) Å in **3**; 1.418(2), 1.429(2) Å in **4**; 1.424(4), 1.433(4) Å in **5HT**) and C−C (1.356(4) Å in **3**; 1.365(2) Å in **4**; 1.368(4) Å in **5HT**) bonds within the planar N-C═C-N fragments are consistent with the dianionic character of the diazabutadiene ligands.[14] The C═C bond of a doubly reduced ene-diamido N-C═C-N moiety also contributes in metal−ligand bonding: η^2-coordination of the ene-diamido moiety to the Yb(III) ion results in the short Yb−C contacts (2.622(3), 2.623(2) Å in **3**; 2.710(2), 2.717(2) Å in **4**; 2.813(3), 2.824(3) Å in **5HT**).

Complexes **2** and **5** coordinated by 2,6-^{i}Pr$_2$C$_6$H$_3$NC(R)C(R)NC$_6$H$_3$^{i}Pr$_2$-2,6 (R = H, Me) ligands turned out to be sensitive to the substituent by the imino carbons: the comparison of their geometric parameters indicates some elongation of Yb−Cp$^{\#}$ bonds (Yb−C$_{aver}$: 2.59 (**2**), 2.62 Å (**5HT**)), while the Yb−N distances remain unchanged. The Yb−C$_{NCCN}$ bonds undergo the most noticeable elongation when replacing H by Me (2.629(5), 2.622(4) Å in **2** vs 2.813(3), 2.824(3) Å in **5HT**). At the same time, the dihedral YbNN−NCCN angle increases from 132.4° (**2**) to 145.4° (**5HT**).

To explore the possibility of a structural phase transition as a consequence of a redox isomerism, the low temperature structure of complex **5** has been studied at 9 K by single-crystal X-ray diffraction (**5LT**). Upon cooling, a subtle disorder−order transition occurs in the case of complex **5LT**, which is accompanied by a space group change from *Pbca* to $P2_1/c$ at 9 K. This structural transition mainly affects the orientation of the coordinated THF molecules and the Cp* ligands and finally emerges in a space group change and the observation of two crystallographically independent molecules of complex **5LT** (Figure 3b,c).

We note that the structural phase transition is accompanied by subtle changes of the coordination behavior of the DAD$^{4i\text{Pr2Me}}$ ligands in **5**. These minute structural changes during the phase transition reflect some systematic trends which might hint for an

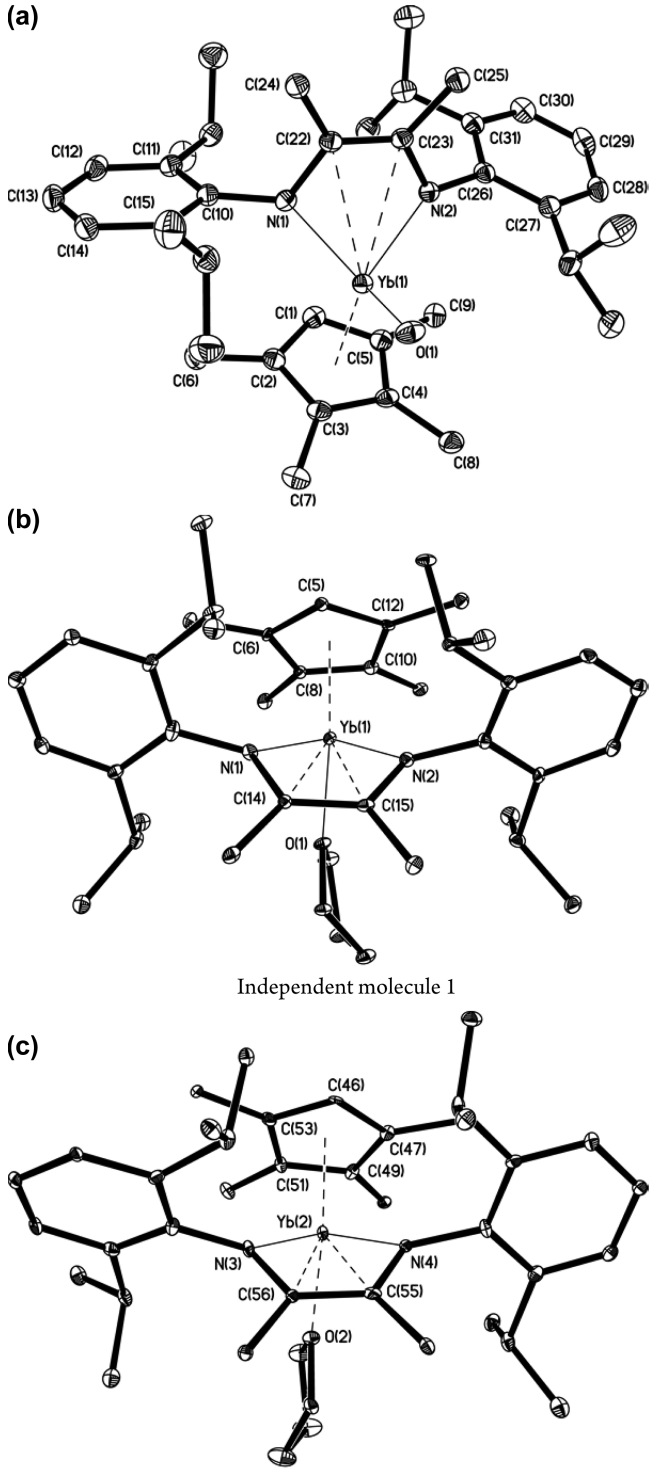

Figure 3. (a) Molecular structure of complex **5HT**. Thermal ellipsoids drawn at the 30% probability level. Carbon atoms of THF molecule and hydrogen atoms are omitted for clarity. (b, c) Molecular structures of complex **5LT** at 9 K showing the orientation of the THF ligands in both crystallographically independent molecules of the low-temperature modification. Thermal ellipsoids drawn at the 30% probability level. Hydrogen atoms are omitted for clarity.

onset of a temperature-induced redox isomerism. Indeed, the low temperature phase of **5LT** differs from its high temperature analogue **5HT** by (*i*) a *shortening* of the N−C bonds of the

DOI: 10.1021/om501121s
Organometallics 2015, 34, 1177−1185

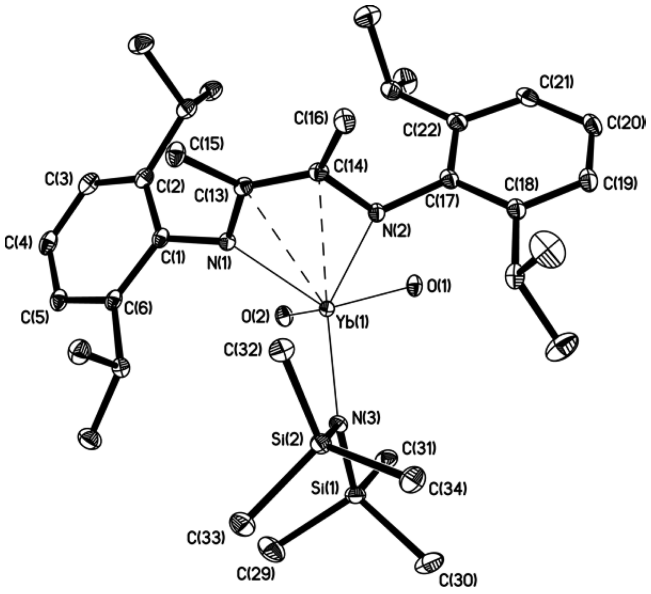

Figure 4. Molecular structure of complex **7**. Thermal ellipsoids drawn at the 30% probability level. Carbon atoms of DME molecules and hydrogen atoms are omitted for clarity.

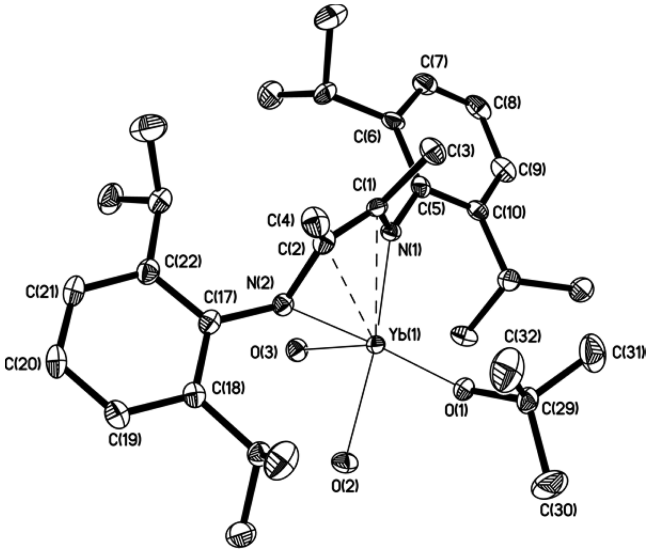

Figure 5. Molecular structure of complex **8**. Thermal ellipsoids drawn at the 30% probability level. Carbon atoms of DME molecule and hydrogen atoms are omitted for clarity.

DAD^{4iPr2Me} ligand (N−C = 1.424(4)−1.433(4) Å for **5HT** and N−C = 1.405(8)−1.419(8) Å for **5LT**) and (*ii*) an *increase* of the Yb−C_{NCCN} bonds (Yb−C = 2.813(3)−2.824(3) Å for **5HT** and Yb−C = 2.825(5)−2.881(6) Å for **5LT**). This observation reveals a slightly increased N═C double bond character of the DAD ligands in **5LT** vs **5HT** and might thus suggest an onset of a redox isomerism which renders **5** from its dianionic form (**5HT**) into the radical-anionic form (**5LT**). This process is also supported by the second structural trend (*increase* of the Yb−C_{NCCN} distances in **5LT**), which reflects the reduced Yb ← σ(C═C) donor and Yb → π^*(C═C) back-donation capabilities of the ene-diamido moiety in **5LT** as a consequence of the starting redox isomerization. Unfortunately, this trend cannot be verified by inspection of the C−C_{NCCN} distances, which remain rather invariant in **5LT** (1.364(8)−1.372(8) Å) and **5HT** (1.368(4) Å). This is caused by the cancellation of two reverse effects: (*i*) shortening of the C−C_{NCCN} bond distances due to reduced interactions between Yb and the ene-diamido moiety in **5LT** and (*ii*) elongation of the C−C bond distances in **5LT** due to the diminished double bond character in the partially radical-anionic form of the DAD ligand relative to **5HT** (dianionic form of the DAD ligand). Numerous trials to detect by X-ray crystallography a structural phase transition for complex **1** whose variable-temperature magnetic properties clearly indicated the existence of redox isomerism[7] have been done. Unfortunately, all the trials failed because of the crystal destruction during cooling to 9 K.

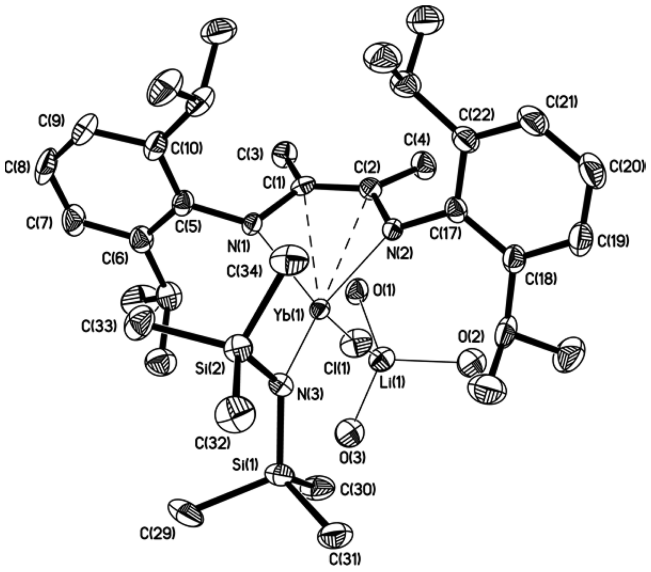

Figure 6. Molecular structure of complex **9**. Thermal ellipsoids drawn at the 30% probability level. Carbon atoms of THF and ether molecules and hydrogen atoms are omitted for clarity.

The monocrystalline samples of complexes **7**, **8** suitable for X-ray analysis were obtained by recrystallization from DME−hexane mixtures, while complex **9** was crystallized from a THF−hexane mixture at ambient temperature. The structures of complexes **7**−**9** were also established by the X-ray diffraction studies. The molecular structures of **7**−**9** are depicted in Figures 4−6, selected bond lengths and angles are given in Table 2, and crystal and structural refinement data are listed in Table S1. In neutral complexes **7** and **8**, the ytterbium ions are coordinated by two nitrogens and two carbons of the DAD^{4iPr2Me} ligand, two oxygens of the DME molecule, and a covalently bonded R-group (R = $N(SiMe_3)_2$ (**7**), O^{t}Bu (**8**)). In *ate*-complex **9**, the coordination sphere of ytterbium is composed by two nitrogen and two carbon atoms of the DAD^{4iPr2Me} ligand and $N(SiMe_3)_2$ amido nitrogen, but instead of a bidentate DME molecule, there is a chloro ligand μ-bridging the Yb and Li ions. The X-ray analysis revealed that, similarly to **3**−**5**, complexes **7**−**9** feature 2σ:η^2-coordination of DAD^{4iPr2Me} ligands; however, the Yb−C_{NCCN} distances detected in complex **7** are essentially longer compared to those of other related complexes (Yb−N bond lengths: 2.169(1), 2.201(1) Å in **7**; 2.152(2), 2.175(2) Å in **8**; 2.139(2), 2.145(2) Å in **9**. Yb−C distances: 2.961(2), 2.975(2) Å in **7**; 2.642(3), 2.644(3) Å in **8**; 2.620(2), 2.624(2) Å in **9**). The geometric parameters of DAD^{4iPr2Me} ligands (C−N bond lengths: 1.432(2), 1.426(2) Å in **7**; 1.424(4), 1.433(4) Å in **8**; 1.415(3), 1.438(3) Å in **9**. C═C bond lengths: 1.356(2) Å in **7**; 1.370(4) Å in **8**, 1.383(4) Å in **9**) are indicative of their dianionic character.

DOI: 10.1021/om501121s
Organometallics 2015, 34, 1177−1185

Table 2. Selected Bond Lengths (Å) and Angles (deg) for Complexes 1−9

complex	Yb−C(Cp) average	Yb−Cp_{Center} or Yb−E (E = N,O)	Yb−N (NCCN)	Yb−C (NCCN)	N−C	C−C (NCCN)	dihedral angle NYbN−NCCN
1	2.59	2.29	2.136(3)	2.628(5)	1.409(5)	1.348(7)	142.2
			2.145(3)	2.618(4)	1.387(6)		
2	2.59	2.29	2.141(3)	2.629(5)	1.411(6)	1.360(6)	134.4
			2.148(3)	2.622(4)	1.406(5)		
3	2.60	2.31	2.151(2)	2.622(3)	1.418(3)	1.356(4)	132.4
			2.151(2)	2.623(2)	1.408(3)		
4	2.61	2.32	2.132(1)	2.710(2)	1.418(2)	1.365(2)	137.6
			2.152(1)	2.717(2)	1.429(2)		
5HT	2.62	2.32	2.139(2)	2.813(3)	1.424(4)	1.368(4)	145.4
			2.151(2)	2.824(3)	1.433(4)		
5LT	2.61	2.32	2.150(6)	2.881(6)	1.417(8)	1.372(8)	150.4
			2.150(5)	2.866(5)	1.415(8)		
7		2.227(1)	2.169(1)	2.961(2)	1.432(2)	1.356(2)	159.5
			2.201(1)	2.975(2)	1.426(2)		
8		2.037(2)	2.152(2)	2.642(3)	1.431(4)	1.370(4)	128.3
			2.175(2)	2.644(3)	1.426(4)		
9		2.220(2)	2.139(2)	2.620(2)	1.415(3)	1.383(4)	126.2
			2.145(2)	2.624(2)	1.438(3)		

The Yb−N, Yb−O, and Yb−Cl bond lengths in complexes **7**−**9** are in line with the trivalent oxidation state of ytterbium atoms in these compounds.[15] It is noteworthy that, in the series of the related compounds $Cp^{\#}Yb^{III}(DAD)^{2-}(thf)$ (**3**−**5**), the values of the dihedral angle NYbN−NCCN vary in the range of 131.2−145.4° depending on the steric demand of both DAD and Cp* ligands. However, for complexes **7**−**9**, the range of variation of this angle is significantly larger: thus, for six-coordinate complex **9**, it is 126.2°, while for seven-coordinate **7** containing the same $N(SiMe_3)_2$ group, this value increases up to 159.5°. The geometry changes appear also in lengthening of Yb−C_{NCCN} distances from 2.620(2) and 2.624(2) Å in **9** to 2.961(2) and 2.975(2) Å in **7**, reflecting weakening of η^2-interaction between Yb and the C═C fragment.

The UV−visible spectra of complexes **3**−**5** and **7**−**9** in THF similarly to $K^+_2[2,6\text{-}R''_2C_6H_3NC(R')C(R')NC_6H_3R''_2\text{-}2,6]^{2-}$ (R′ = H, Me; R″ = Me, ^{i}Pr) show strong absorptions in the region λ = 280−290 nm characteristic for dianionic diazabutadiene ligands (see Figures S10−13, Supporting Information). The ^{1}H NMR spectra of complexes **3**−**5** and **7**−**9** (C_6D_6, 20 °C) exhibit the signals in the range from −130 to 130 ppm and are indicative of a trivalent oxidation state of ytterbium in these compounds (see Figures S10−13). Thereby, the spectroscopic data of complexes **3**−**5** and **7**−**9** are consistent with the Yb(III) derivatives coordinated by dianionic diazabutadiene ligands.

Magnetic Measurements. Magnetic measurements of crystalline samples **3**−**5** and **7**−**9** have been carried out by using an MPMS-XL SQUID magnetometer in the temperature range of 1.8−300 K with an applied magnetic field of 1000 Oe. The temperature dependences of the χT product (or magnetic moment) for all of these samples present a relatively simlar shape and characteristic of the presence of paramagnetic Yb(III) and diamagnetic ligands (Figure 7a,b).

Indeed, the Yb(III) ion has a $^2F_{7/2}$ ground state with a first-order orbital momentum.[16] In the low symmetry site, as it may be expected for all described compounds, this state is split into Stark components by the crystal field, each of them being a Kramers doublet. At room temperature, the excited states of the $^2F_{7/2}$ of Yb(III) ion are populated and the theoretical Yb(III) free-ion value of χT is equal to 2.49 cm^3 K mol^{-1}(4.46 μ_B). At 300 K, the

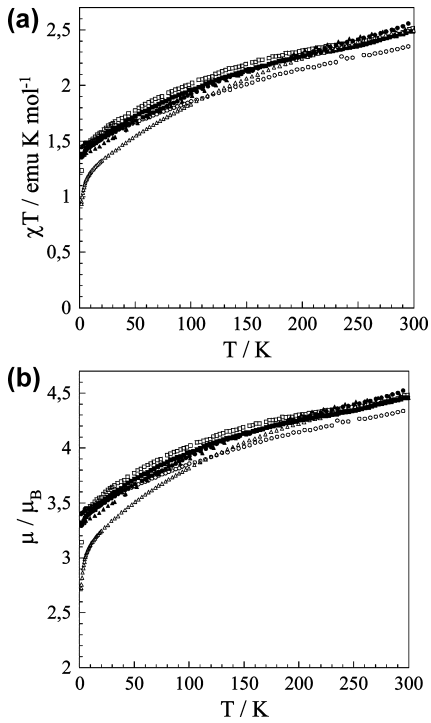

Figure 7. (a) χT vs T curves performed at an applied magnetic field of 1000 Oe for **3** (▶), **4** (□), **5** (■), **7** (●), **8** (○), **9** (Δ). (b) Magnetic moment vs T curves performed at an applied magnetic field of 1000 Oe for **3** (▶), **4** (□), **5** (■), **7** (●), **8** (○), **9** (Δ).

observed χT values for all compounds are in the range 2.38−2.56 cm^3 K mol^{-1} or 4.36−4.52 μ_B (**3**: 2.48 cm^3 K mol^{-1} (4.45 μ_B); **4**: 2.51 cm^3 K mol^{-1} (4.48 μ_B); **5**: 2.49 cm^3 K mol^{-1} (4.46 μ_B); **7**: 2.38 cm^3 K mol^{-1} (4.36 μ_B); **8**: 2.56 cm^3 K mol^{-1} (4.52 μ_B)); **9**: 2.49 cm^3 K mol^{-1} (4.47 μ_B)), which is close to the expected value for paramagnetic Yb(III). Therefore, this confirms that the ligand is diamagnetic.

As the temperature decreases, χT for all curves decreases, and at 1.8 K, it reaches the values comprised in the range of 0.93−1.44 cm^3 K mol^{-1} (2.72−3.39 μ_B). Such a decrease can be explained by the depopulation of the Stark levels of Yb(III)

DOI: 10.1021/om501121s
Organometallics 2015, 34, 1177−1185

ground state: at room temperature, the excited states of Yb(III) ion are populated, but as the temperature decreases, there is the progressive depopulation of the excited Kramers doublets, and at low temperature, only the ground Kramers doublet is populated. The lower χT value observed for sample **9** may be explained by slightly different symmetry of this complex, which induces the difference in the thermal depopulation phenomenon.

Formerly, we reported on unusual magnetic behavior of **1** indicative of the existence of thermally induced redox isomerism for this compound. Thus, the value of magnetic moment at T = 300 K is 4.41 μ_B, which is close to the calculated free Yb(III) ion value for a $^2F_{7/2}$ multiplet and corresponds to the $[Cp^*Yb^{III}(DAD)^{2-}(thf)]$ form. The value of the magnetic moment of **1** at T = 2 K of 2.03 μ_B is too low for Yb(III) and is more compatible with the magnetic moments observed for organic radical anions with spin $S = 1/2$ (1.73 μ_B) consistent with $[Cp^*Yb^{II}(DAD)^{-}(thf)]$ isomer. Surprisingly the related Yb(III) complexes **3**−**5**, **7**−**9** coordinated by dianionic diazabutadiene ligands and having the similar structures do not feature the similar magnetic behavior in the broad temperature interval: with temperature decrease, their magnetic moments do not drop to such a low value and remain within the range characteristic for Yb(III) species and behave as isolated paramagnets.

SUMMARY AND CONCLUSIONS

The electrochemical measurements performed for a series of bulky DADs demonstrated that the alkyl groups in the aromatic substituents by the nitrogens have negligible influence on the reduction potential values, while the introduction of methyl groups at the imine carbon atoms substantially modifies these values. Thus, DAD^{4Me2H} and DAD^{4iPr2H} are more readily reduced than their Me-substituted analogues for approximately 400 mV. It was found that the reactions of $Cp^{\#}{}_2Yb(THF)_2$ ($Cp^{\#}$ = C_5Me_5, C_5Me_4H) with diazabutadienes 2,6-$R''{}_2C_6H_3N{=}C(R')$-$C(R'){=}NC_6H_3R''{}_2$-2,6 (R′ = H, Me; R″ = Me, ^{i}Pr) afford complexes $Cp^{\#}Yb^{III}(DAD)^{2-}(thf)$ regardless of the different steric bulk of the substituents by the nitrogens (2,6-$^i Pr_2C_6H_3$− and 2,6-$Me_2C_6H_3$). The variation of redox properties of the DAD ligands due to the change of the substituents by the imino carbons (Me vs H) also does not affect the reactions outcome. The X-ray studies of complexes **3**−**5** and **7**−**9** revealed that they feature the $2\sigma{:}\eta^2$-type of coordination of dianionic DAD ligands. The Me-substituents by the imino carbons of DADs lead to some elongation of Yb−$Cp^{\#}$ bonds. The Yb−C_{NCCN} bonds and the dihedral YbNN−NCCN angles were found to be the most sensitive to replacing H by Me. A synthetic approach to the amido and alkoxo Yb(III) complexes supported by the dianionic $[2,6\text{-}^iPr_2C_6H_3NC(Me)C(Me)NC_6H_3{}^iPr_2\text{-}2,6]^{2-}$ ligand was developed. For complex **5** at 9 K, the structural phase transition accompanied by subtle changes of the coordination behavior of the $DAD^{4iPr2Me}$ ligand was detected. These structural changes during the phase transition reflect some systematic trends which might hint for an onset of a temperature-induced redox isomerism. Thermally induced redox isomeric transformations in Yb(III) complexes coordinated by the dianionic diazabutadiene ligand were demonstrated to be very subtle processes highly sensitive to the changes in steric and redox properties of the DAD ligand and those of the redox innocent ligand coordinated to the Yb(III) center.

The further studies on the synthesis of Yb(III) and Yb(II) complexes containing various N,N redox active ligands and investigation of their structural and magnetic properties are pursued in our groups.

EXPERIMENTAL SECTION

General Considerations and Materials Characterization. All experiments were performed in evacuated tubes, using standard Schlenk-tube and glovebox techniques, with rigorous exclusion of traces of moisture and air. After drying over KOH, THF was purified by distillation from sodium/benzophenone ketyl and hexane and toluene by distillation from sodium/triglyme benzophenone ketyl prior to use. $(C_5Me_5)_2Yb(thf)_2$,[17] $(C_5Me_4H)_2Yb(thf)_2$,[18] anhydrous $YbCl_3$[19] and 2,6-$R''{}_2C_6H_3N{=}C(R')$-$C(R'){=}NC_6H_3R''{}_2$-2,6 (R′ = H, Me; R″ = Me, ^{i}Pr)[20] and $(Me_3Si)_2NLi(Et_2O)$[21] were prepared according to literature procedures. ^{t}BuOK and $(Me_3Si)_2NNa$ were purchased from Acros and were used without further purification. All other commercially available chemicals were used after the appropriate purification. IR spectra were recorded as Nujol mulls on a Bruker-Vertex 70 spectrophotometer. A "Polaris Q GC/MS" spectrometer was used for GS/MS analysis. NMR spectra were recorded with Bruker Avance DRX-400 and Bruker DRX-200 spectrometers in C_6D_6 at 20 °C, unless otherwise stated. Chemical shifts for ^{1}H and ^{13}C NMR spectra were referenced internally to the residual solvent resonances and are reported relative to TMS. The C, H, N elemental analysis was carried out in the microanalytical laboratory of IOMC. Lanthanide metal analyses were carried out by complexometric titration.[22]

Synthesis of $(C_5Me_4H)Yb(^{4Me2H}DAD)(thf)$ (3). A solution of ^{4Me2H}DAD (0.30 g,1.14 mmol) in thf (5 mL) was added to a solution of $(C_5Me_4H)_2Yb(thf)_2$ (0.64 g, 1.14 mmol) in thf (10 mL). The reaction mixture was stirred for 0.5 h at 40 °C. After removal of thf in vacuum, toluene (15 mL) was added and the solution was heated at 60 °C for 5 h. The volatiles were evaporated in vacuum (80 °C) and collected. Recrystallization of the solid residue from hexane (−5 °C) gave **3** as yellowish green crystals (0.36 g, 49%). The crystals were washed with cold hexane and dried in vacuum at room temperature for 15 min. In the condensate, 0.10 g (78%) of $C_5Me_4H_2$ was detected by GC. ^{1}H NMR (400 MHz, C_6D_6, 293 K): δ −48.58 (s, 2H, NCHCHN), −21.83 (s, 2H, CH Ar), −12.09 (s, 6H, $(CH_3)_2$Ar), −8.34 (s, 2H, CH Ar), −4.93 (s, 6H, $C_5(CH_3)_4H$), 1.28 (s, 1H, $C_5(CH_3)_4H$), 4.39 (s, 6H, $C_5(CH_3)_4H$), 6.93 (s, 2H, CH Ar), 34.84 (s, 4H, C_4H_8O), 40.62 (s, 6H, $(CH_3)_2$Ar), 93.13 (s, 4H, C_4H_8O). IR (Nujol, KBr, cm^{-1}): 1589 (m), 1273 (s), 1197 (s), 1123(m), 1093(s), 1011(m), 858(m), 763 (m), 577 (m). Anal. Calcd for $C_{31}H_{41}N_2OYb$: C, 59.04; H, 6.54; N, 4.44; Yb, 27.43. Found: C, 58.52; H, 6.11; N, 4.02; Yb, 27.77.

Synthesis of $(C_5Me_5)Yb(^{4Me2Me}DAD)(thf)$ (4). A solution of ^{4Me2Me}DAD (0.40 g, 1.37 mmol) in thf (5 mL) was added to a solution of $(C_5Me_5)_2Yb(THF)_2$ (0.80 g, 1.36 mmol) in thf (20 mL). The reaction mixture was stirred for 0.5 h at 40 °C. After removal of thf in vacuum, toluene (15 mL) was added and the solution was heated at 60 °C for 5 h. The volatiles were evaporated in vacuum (80 °C) and collected. Recrystallization of the solid residue from hexane (−5 °C) gave **4** as yellowish green crystals (0.52 g, 57%). The crystals were washed with cold hexane and dried in vacuum at room temperature for 15 min. In the condensate, 0.10 g (52%) of C_5Me_5H was detected by GC. ^{1}H NMR (400 MHz, C_6D_6, 293 K): −59.87 (s, 6H, NC(CH_3)-C(CH_3)N), −16.43 (s, 2H, CH Ar), −11.47 (s, 6H, $(CH_3)_2$Ar), −5.26 (s, 2H, CH Ar), −4.43 (s, 6H, $(CH_3)_2$Ar), −0.43 (s, 2H, CH Ar), 6.10 (s, 15H, $C_5(CH_3)_5$), 7.03 (s, 4H, C_4H_8O), 57.18 (s, 4H, C_4H_8O). IR (Nujol, KBr, cm^{-1}): 1588 (s), 1269 (s), 1199 (m), 1148 (m), 1096(m), 1008 (m), 857 (m), 805 (m), 761 (m), 577 (m). Anal. Calcd for $C_{34}H_{47}N_2OYb$: C, 60.70; H, 7.03; N, 4.16; Yb, 25.72. Found: C, 60.24; H, 6.79; N, 4.00; Yb, 25.99.

Synthesis of $(C_5Me_4H)Yb(^{4iPr2Me}DAD)(thf)$ (5) and $(C_5Me_4H)_3Yb$ (6). A solution of ^{4iPr2Me}DAD (0.36 g, 0.89 mmol) in THF (5 mL) was added to a solution of $(C_5Me_4H)_2Yb(thf)_2$ (0.54 g, 0.96 mmol) in thf (10 mL). The reaction mixture was stirred for 0.5 h at 40 °C. After removal of thf in vacuum, toluene (15 mL) was added and the solution was heated at 60 °C for 4 h. The volatiles were evaporated in vacuum (80 °C) and collected. Recrystallization of the solid residue from hexane (−5 °C) gave the mixture of yellow and dark maroon crystals. Fractional crystallization afforded yellowish green crystals of **5** (0.26 g, 35%) and dark maroon crystals (0.05 g, 10%) of **6**. In the condensate, 0.07 g (64%) of $C_5Me_4H_2$ was detected by GC. **5**: ^{1}H NMR

DOI: 10.1021/om501121s
Organometallics 2015, 34, 1177−1185

(400 MHz, C_6D_6, 293 K): −108.23 (s, 2H, $CH(CH_3)_2$); −43.6 (s, 6H, $NC(CH_3)$), −18.44 (s, 2H, CH Ar), −14.00 (s, 6H, $CH(CH_3)_2$), −8.53 (s, 2H, $CH(CH_3)_2$), −8.09 (s, 6H, $CH(CH_3)_2$), −6.94 (s, 2H, CH Ar), −2.27 (s, 6H, $C_5(CH_3)_4H$), −0.63 (s, 2H, CH Ar), 1.36 (s, 6H, $C_5(CH_3)_4H$), 7.02 (s, 1H, $C_5(CH_3)_4H$), 20.43 (s, 6H, $CH(CH_3)_2$), 36.10 (s, 6H, $CH(CH_3)_2$), 58.63 (s, 4H, C_4H_8O), 125.48 (s, 4H, C_4H_8O). IR (Nujol, KBr, cm^{-1}): 1591 (s), 1267 (s), 1183 (m), 1122 (s), 1043 (m), 937 (m), 765 (m), 523 (m). Anal. Calcd for $C_{41}H_{61}N_2OYb$: C, 63.82; H, 7.96; N 3.63; Yb, 22.44. Found: C, 63.41; H, 7.80; N, 3.23; Yb 22.59. **6**: IR (Nujol, KBr, cm−1) 1326 (m), 1149 (s), 1019 (m), 969 (m), 608 (m). Anal. Calcd for $C_{29}H_{37}Yb$: C, 64.85; H, 6.90; Yb, 27.43. Found: C, 64.49; H, 7.15; Yb, 27.59.

Synthesis of $(Me_3Si)_2Yb(DAD^{4iPr2Me})(dme)$ (7). A solution of $DAD^{4iPr2Me}$ (0.80 g, 1.98 mmol) in thf (20 mL) was added to Na shavings (0.09 g, 3.96 mmol), and the reaction mixture was stirred at room temperature for 3 days until complete dissolution of the metal. The resulting dark-red solution was filtered and added slowly to a solution of (1.98 mmol) $((Me_3Si)_2N)YbCl_2(THF)_n$, which was obtained *in situ* from $YbCl_3$ (0.55 g, 1.98 mmol) and $NaN(SiMe_3)_2$ (0.36 g, 1.98 mmol) in thf (15 mL) (60 °C, 72 h). The reaction mixture was stirred at room temperature for 2 days (20 °C). The resulting brownish-green solution was filtered, the volatiles were evaporated in vacuum, the resulting solid residue was extracted with toluene (25 mL), and the extracts were filtered. Toluene was then evaporated in vacuum. Recrystallization of the solid residue from a DME−hexane (1:3) mixture (20 °C) afforded **7** as blue green crystals (0.72 g, 44%). IR (Nujol, KBr, cm^{-1}): 1583 (s), 1252 (s), 1202 (s), 1120 (m), 1091 (m), 1043 (m), 826 (m), 763 (m), 670 (m). Anal. Calcd for $C_{38}H_{68}N_3O_2Si_2Yb$: C, 55.06; H, 8.21; N, 5.07; Yb, 20.89; found: C, 55.83; H, 8.01; N, 5.99; Yb, 21.07.

Synthesis of $(^tBuO)Yb(DAD^{4iPr2Me})(dme)$ (8). A solution of $DAD^{4iPr2Me}$ (0.88 g, 2.18 mmol) in THF (20 mL) was added to an excess of Na shavings (0.10 g, 4.36 mmol), and the reaction mixture was stirred at room temperature for 3 days until complete dissolution of the metal. The resulting dark-red solution was filtered and added slowly to a solution of (2.18 mmol) $(^tBuO)YbCl_2(THF)_n$, which was obtained *in situ* from $YbCl_3$ (0.61 g, 2.18 mmol) and ^tBuOK (0.24 g, 2.18 mmol) in THF (15 mL) (60 °C, 72 h). The reaction mixture was stirred at room temperature for 2 days (20 °C). The resulting brownish-green solution was filtered, the solvent was evaporated in vacuum, the resulting solid residue was extracted with toluene (25 mL), and the extracts were filtered. Toluene was then evaporated in vacuum. Recrystallization of the solid residue from a DME−hexane (1:4) mixture (20 °C) afforded **8** as blue green crystals (0.93 g, 58%). IR (Nujol, KBr, cm^{-1}):1589 (s), 1269 (s), 1210 (s), 1197 (m), 1148 (m), 1088 (s), 1029 (m), 825 (m), 793 (m), 752 (m), 696 (m), 553 (m). Anal. Calcd for $C_{36}H_{59}N_2O_3Yb$: C, 58.31; H, 7.96; N, 3.78; Yb, 23.36; found: C, 57.95; H, 8.09; N, 3.99; Yb 23.83.

Synthesis of $\{Li(thf)_3\}\{Yb[^{4iPr2Me}DAD][N(SiMe_3)_2](\mu\text{-}Cl)\}$ (9). A solution of $^{4iPr2Me}DAD$ (0.57 g, 1.41 mmol) in THF (20 mL) was added to Li shavings (0.02 g, 2.82 mmol), and the reaction mixture was stirred at room temperature for 3 days until complete dissolution of the metal. The resulting dark-red solution was filtered and added slowly to a solution of (1.41 mmol) $[(Me_3Si)_2N]YbCl_2(THF)_n$, which was obtained *in situ* from $YbCl_3$ (0.39 g, 1.41 mmol) and $LiN(SiMe_3)_2(Et_2O)$ (0.34 g, 1.41 mmol) in THF (15 mL) (60 °C, 72 h). The reaction mixture was stirred at room temperature for 2 days. The solvent was evaporated in vacuum, and the resulting solid residue was extracted with toluene (25 mL). Recrystallization from a THF−hexane mixture afforded **9** as blue green crystals (0.59 g, 42%). IR (Nujol, KBr, cm^{-1}):1586 (s), 1249(s), 1115(s), 1038(s), 937 (m), 887 (m), 773 (m), 728 (m), 561 (s), 527 (s). Anal. Calcd for $C_{46}H_{83}ClLiN_3O_3Si_2Yb$: C, 55.32; H, 8.32; N, 4.21; Yb, 17.34; found: C, 55.00; H, 8.13; N, 3.99; Yb 18.07.

Electrochemical Studies. Electrochemical studies were carried out using an IPC-Win digital potentiostat/galvanostat connected to a PC. Voltammograms were recorded by cyclic voltammetry (CV) at a stationary Pt disk electrode (d = 3.2 mm) at different potential scan rates in DMF using a 0.05 M n-Bu_4NBF_4 solution as the supporting electrolyte at 20 °C in a 10 mL electrochemical cell. Oxygen was removed from the cell by purging with dry argon. Platinum wire served as the auxiliary electrode, and a saturated silver chloride electrode was used as the reference electrode. The potential of the Fc/Fc^+ redox couple in our experimental conditions is +0.53 V.

Crystal Structure Determination of 3−9. X-ray diffraction intensity data for compounds **3**−**9** were collected on Bruker Smart APEX-II (**3**) and Bruker Smart APEX (**4**, **5HT**, **6**−**9**) diffractometers with graphite monochromated Mo−Kα radiation (λ = 0.71073 Å) using ω scans. The structures were solved by direct methods and were refined on F^2 using the SHELXTL package.[23] All non-hydrogen atoms were found from Fourier syntheses of electron density and were refined anisotropically. All hydrogen atoms were placed in calculated positions and were refined in the riding model with $U_{iso}(H)$ = 1.2 U_{eq} ($U_{iso}(H)$ = 1.5 U_{eq} for the hydrogen atoms in CH_3 groups) of their parent atoms. SADABS[24] was used to perform area-detector scaling and absorption corrections.

A crystal of **5LT** was glued under an inert gas atmosphere on a MiTeGenMicroMount, mounted on a Huber 4-circle diffractometer equipped with a 4K-Displex closed-cycle helium cryostat and was cooled to 9(1) K. Preliminary examination and final data collection were carried out with graphite-monochromated Mo Kα radiation (λ = 0.71073 Å) generated from a Bruker FR 591 rotating anode running at 50 kV and 60 mA. Intensity data were collected employing a MAR345 IP Detector and 1° φ-scans with a detector-to-sample distance of 160 mm.

The systematic pseudo-merohedrically twining of the crystals of **5LT** afforded an empirical absorption correction using the program TWINABS[25] (T_{min} = 0.3195, T_{max} = 0.4305) for a total of 58 914 reflections and 15 169 unique reflections (R_{int} = 0.0214). For the refinements, a HKLF5 formatted data file with 29 621 reflections was used. Subsequent full-matrix least-squares refinements against F^2 were carried out using the SHELXL97 program.[26] All non-hydrogen atoms were found from Fourier syntheses of electron density and were refined anisotropically. All hydrogen atoms were placed in geometrically idealized positions and treated as riding with $U_{iso}(H)$ = 1.2 U_{eq} ($U_{iso}(H)$ = 1.5 U_{eq} for the hydrogen atoms in CH_3 groups) of their parent atoms. Due to strong correlation between the parameters of the two crystallographically independent molecules in the unit cell, it was necessary to restrain the displacement parameters of seven atoms to be isotropic. A batch scaling factor was introduced to describe the twin volume fractions, resulting in a 0.6813/0.3187 ratio for the volume of domains 1 and 2, respectively. Low values of completeness (90.8% for θ = 26° and 85.6% for θ = 25°) are explained by poor quality of the crystal specimen.

Crystal data and details of data collection and structure refinement for the different compounds are given in Table S1 (Supporting Information). Main crystallographic data (excluding structure factors) are available as Supporting Information, as CIF files. CCDC-1024539 (**3**), 1024540 (**4**), 1024541 (**5LT**), 1024542 (**5HT**), 1031761 (**6**), 1024543 (**7**), 1024544 (**8**), and 1024545 (**9**) contain the supplementary crystallographic data for this paper; crystallographic data for **1** and **2** were previously published[7] as CCDC-607546 (**1**) and 607547 (**2**). These data can be obtained free of charge via ccdc.cam.ac.uk/community/requestastructure.

Magnetic Measurements. Magnetic susceptibility data were collected with a Quantum Design MPMS-XL SQUID magnetometer working between 1.8 and 350.0 K with the magnetic field up to 7 T. The samples were prepared in a glow box and kept in an anaerobic atmosphere. The magnetic data were corrected for the sample holder, and the diamagnetic contributions were calculated from the Pascal's constants.[27]

■ ASSOCIATED CONTENT

Supporting Information

CV curves, molecular structure, table of crystallographic data and structure refinement details, IR spectra, UV/vis spectra, and ^1H NMR spectra. This material is available free of charge via the Internet at http://pubs.acs.org.

DOI: 10.1021/om501121s
Organometallics 2015, 34, 1177−1185

AUTHOR INFORMATION

Corresponding Author

*E-mail: trif@iomc.ras.ru. Fax: (+7)8314621497 (A.A.T.).

Notes

The authors declare no competing financial interest.

ACKNOWLEDGMENTS

This work was supported by the Russian Foundation for Basic Research grants 13-03-97027 and 14-03-31281 mol_a, by the grant of The Ministry of Education and Science of the Russian Federation (the agreement of August 27, 2013 No. 02.B.49.21.0003 between The Ministry of Education and Science of the Russian Federation and Lobachevsky State University of Nizhni Novgorod). We thank Synor Ltd. and personally Dr. A. Tatarnikov for donation of C_5Me_5H and $C_5Me_4H_2$.

REFERENCES

(1) van Koten, G.; Vrieze, K. *Adv. Organomet. Chem.* **1982**, *21*, 151−239.

(2) Trifonov, A. A. *Eur. J. Inorg. Chem.* **2007**, 3151−3167.

(3) (a) Moore, J. A.; Cowley, A. H.; Gordon, J. C. *Organometallics* **2006**, *25*, 5207−5209. (b) Vasudevan, K.; Cowley, A. H. *Chem. Commun.* **2007**, 3464−3466.

(4) (a) tom Dieck, H.; Renk, I. W. *Chem. Ber.* **1971**, *104*, 110−130. (b) tom Dieck, H.; Franz, K.-D.; Hoffmann, F. *Chem. Ber.* **1975**, *108*, 163−173. (c) Reinhold, J.; Benedix, R.; Birner, P.; Hennig, H. *Inorg. Chim. Acta* **1979**, *33*, 209−213.

(5) (a) Morss, L. R. *Chem. Rev.* **1976**, *76*, 827−841. (b) Finke, R. G.; Keenan, S. R.; Shirardi, D. A.; Watson, P. L. *Organometallics* **1986**, *5*, 598−601. (c) Bond, A. M.; Deacon, G. B.; Newnham, R. H. *Organometallics* **1986**, *5*, 2312−2316.

(6) (a) Trifonov, A. A.; Kirillov, E. N.; Bochkarev, M. N.; Schumann, H.; Muehle, S. *Russ. Chem. Bull.* **1999**, *48*, 382−384. (b) Trifonov, A. A.; Kurskii, Yu. A.; Bochkarev, M. N.; Muehle, S.; Dechert, S.; Schumann, H. *Russ. Chem. Bull.* **2003**, *52*, 601−606. (c) Trifonov, A. A.; Fedorova, E. A.; Ikorskii, V. N.; Dechert, S.; Schumann, H.; Bochkarev, M. N. *Eur. J. Inorg. Chem.* **2005**, 2812−2818. (d) Trifonov, A. A.; Fedorova, E. A.; Fukin, G. K.; Ikorskii, V. N.; Kurskii, Yu. A.; Dechert, S.; Schumann, H.; Bochkarev, M. N. *Russ. Chem. Bull.* **2004**, *53*, 2736−2743. (e) Wang, J.; Amos, R. I. J.; Frey, A. S. P.; Gardiner, M. G. *Organometallics* **2005**, *24*, 2259−2261. (f) Cui, P.; Chen, Y.; Wang, G.; Li, G.; Xia, W. *Organometallics* **2008**, *27*, 4013−4016. (g) Walter, M. D.; Berg, D. J.; Andersen, R. A. *Organometallics* **2007**, *26*, 2296−2307. (h) Booth, C. H.; Walter, M. D.; Kazhdan, D.; Hu, Y.-J.; Lukens, W. W.; Bauer, E. D.; Maron, L.; Eisenstein, O.; Andersen, R. A. *J. Am. Chem. Soc.* **2009**, *131*, 6480−6491.

(7) Trifonov, A. A.; Borovkov, I. A.; Fedorova, E. A.; Fukin, G. K.; Larionova, J.; Druzhkov, N. O.; Cherkasov, V. K. *Chem.—Eur. J.* **2007**, *13*, 4981−4987.

(8) Fedushkin, I. L.; Maslova, O. V.; Morozov, A. G.; Dechert, S.; Demeshko, S.; Meyer, F. *Angew. Chem., Int. Ed.* **2012**, *51*, 10584−10587.

(9) (a) Trifonov, A. A.; Fedorova, E. A.; Fukin, G. K.; Druzhkov, N. O.; Bochkarev, M. N. *Angew. Chem., Int. Ed.* **2004**, 5045−5048. (b) Trifonov, A. A.; Fedorova, E. A.; Fukin, G. K.; Baranov, E. V.; Druzhkov, N. O.; Bochkarev, M. N. *Chem.—Eur. J.* **2006**, *12*, 2752−2757.

(10) Trifonov, A. A.; Shestakov, B. G.; Lyssenko, K. A.; Larionova, J.; Fukin, G. K.; Cherkasov, A. V. *Organometallics* **2011**, *30*, 4882−4889.

(11) Allan, C. J.; Cooper, B. F. T.; Cowley, H. J.; Rawson, J. M.; Macdonald, C. L. B. *Chem.—Eur. J.* **2013**, *19*, 14470−14483.

(12) Tilley, D.; Andersen, R. A.; Spencer, B.; Zalkin, A. *Inorg. Chem.* **1982**, *21*, 2647−2649.

(13) (a) Pi, C.; Zhu, Z.; Weng, L.; Chen, Z.; Zhou, X. *Chem. Commun.* **2007**, 2190−2192. (b) Mao, L.; Shen, Q.; Jin, S. *Polyhedron* **1994**, *13*, 1023−1025. (c) Wang, Y.; Shen, Q.; Xue, F.; Yu, K. *J. Organomet. Chem.* **2000**, *598*, 359−364.

(14) For standard C−C and C−N bond lengths, see: Allen, A.; Konnard, O.; Watson, D. G.; Brammer, L.; Orpen, G.; Taylor, R. *J. Chem. Soc., Perkin Trans.* **1987**, 1−19.

(15) For comparison, see: (a) Deacon, G. B.; Forsyth, C. M.; Scott, N. M. *Dalton Trans.* **2003**, 3216−3229. (b) Hou, Z.; Koizumi, T.; Nishiura, M.; Wakatsuki, Y. *Organometallics* **2001**, *20*, 3323−3328. (c) Hao, J.; Song, H.; Cui, C. *Organometallics* **2001**, *20*, 3323−3328.

(16) Carlin, R. L. *Magnetochemistry*; Springer-Verlag: Berlin, 1986.

(17) Watson, P. L. *J. Chem. Soc., Chem. Commun.* **1980**, 652−653.

(18) Zinnen, H. A.; Pluth, J. J.; Evans, W. J. *J. Chem. Soc., Chem.Commun.* **1980**, 810−812.

(19) Taylor, M. D.; Carter, C. P. *J. Inorg. Nucl. Chem.* **1962**, *24*, 387−391.

(20) Svoboda, M.; Dieck, H. T. *J. Organomet. Chem.* **1980**, *191*, 321−327.

(21) Manzer, L. E. *Inorg. Chem.* **1978**, *17*, 1552−1558.

(22) Lyle, S. J.; Rahman, M. M. *Talanta* **1953**, *10*, 1177−1182.

(23) Sheldrick, G. M. *SHELXTL v.6.12: Structure Determination Software Suite*; Bruker AXS: Madison, WI, 2000.

(24) Sheldrick, G. M. *SADABS v.2.01: Bruker/Siemens Area Detector Absorption Correction Program*; Bruker AXS: Madison, WI, 1998.

(25) Sheldrick, G. M. *TWINABS*; Bruker AXS: Madison, WI, 2001.

(26) Sheldrick, G. M. *Acta Crystallogr.* **2008**, *A64*, 112−122.

(27) Boudreaux, E. A.; Mulay, L.; Sons, L. J. W. *Theory and Applications of Molecular Paramagnetism*; Wiley: New York, 1976.

DOI: 10.1021/om501121s
Organometallics 2015, 34, 1177−1185